


Collapsin response mediator protein 2: high-resolution crystal structure sheds light on small-molecule binding, post-translational modifications, and conformational flexibility

Matti Myllykoski¹ · Anne Baumann^{2,3} · Kenneth Hensley⁴ · Petri Kursula^{1,2} 

Received: 15 December 2016 / Accepted: 19 December 2016 / Published online: 2 January 2017
© Springer-Verlag Wien 2016

Abstract Collapsin response mediator protein 2 (CRMP-2) is a neuronal protein involved in axonal pathfinding. Intense research is focusing on its role in various neurological diseases. Despite a wealth of studies, not much is known about the molecular mechanisms of CRMP-2 function in vivo. The detailed structure–function relationships of CRMP-2 have also largely remained unknown, in part due to the fact that the available crystal structures lack the C-terminal tail, which is known to be a target for many post-translational modifications and protein interactions. Although CRMP-2, and other CRMPs, belong to the dihydropyrimidinase family, they have lost the enzymatic active site. Drug candidates for CRMP-2-related processes have come up during the recent years, but no reports of CRMP-2 complexes with small molecules have emerged. Here, CRMP-2 was studied at 1.25-Å resolution using X-ray crystallography. In addition, ligands were docked into the homotetrameric structure, and the C-terminal tail of CRMP-2 was produced recombinantly and analyzed. We have obtained the human CRMP-2 crystal structure at atomic resolution and could identify small-molecule binding pockets in the protein. Structures obtained in different crystal forms highlight flexible regions near possible

ligand-binding pockets. We also used the CRMP-2 structure to analyze known or suggested post-translational modifications at the 3D structural level. The high-resolution CRMP-2 structure was also used for docking experiments with the sulfur amino acid metabolite lanthionine ketimine and its ester. We show that the C-terminal tail is intrinsically disordered, but it has conserved segments that may act as interaction sites. Our data provide the most accurate structural data on CRMPs to date and will be useful in further computational and experimental studies on CRMP-2, its function, and its binding to small-molecule ligands.

Keywords Axonal pathfinding · Protein structure · Ligand docking · Intrinsic disorder · X-ray crystallography · Lanthionine ketimine

Background

Five collapsin response mediator proteins (CRMP) have been characterized, and they have similar properties, being able to form homo- and heterotetramers (Wang and Strittmatter 1997). Structurally, the CRMPs are homologous to the family of dihydropyrimidinases (DHPase), but the catalytic residues are not conserved (Wang and Strittmatter 1997; Stenmark et al. 2007; Ponnusamy and Lohkamp 2013). The only reported catalytic activity concerns a histone deacetylase activity in CRMP-3 (Hou et al. 2013).

CRMP-2 is a cytosolic tetrameric protein with important roles in e.g. axonal growth and guidance (Khanna et al. 2012). The C-terminal tail of CRMP-2 bears remarkable similarity to the tau protein at the molecular level (Hensley and Kursula 2016), suggesting possible involvement in neurodegenerative disease. Recent knock-out mouse studies have further highlighted the relevance of CRMP-2 for

✉ Petri Kursula
petri.kursula@uib.no

¹ Faculty of Biochemistry and Molecular Medicine and Biocenter Oulu, University of Oulu, Oulu, Finland

² Department of Biomedicine, University of Bergen, Bergen, Norway

³ Division of Psychiatry, Haukeland University Hospital, Bergen, Norway

⁴ Arkansas College of Osteopathic Medicine, Fort Smith, AR, USA

both normal neurodevelopment and neuropsychiatric conditions (Makihara et al. 2016; Nakamura et al. 2016; Zhang et al. 2016).

A number of binding partners for CRMP-2 have been reported, including tubulin (Fukata et al. 2002; Kimura et al. 2005), calmodulin (CaM) (Zhang et al. 2009), phospholipase D2 (Lee et al. 2002), proline-rich inositol polyphosphate 5-phosphatase (Aistle et al. 2011), and ceroid-lipofuscinosis neuronal protein 6 (Benedict et al. 2009). Interactions with ion channels have also been reported (Chi et al. 2009; Piekarz et al. 2012). CRMP-2 is a target of phosphorylation by several kinases (Gu et al. 2000; Uchida et al. 2009; Brittain et al. 2012; Wilson et al. 2014). The function of CRMP-2 at the molecular level, however, is still largely unknown. The apparent lack of catalytic activity and the tetrameric oligomeric state suggest a role as an interaction hub or a molecular scaffold binding to components of both the cytoskeleton and the neuronal plasma membrane.

In recent years, CRMP-2 has emerged as a potential drug target for neurological diseases (Hensley et al. 2011). Currently studied drug candidates with relevance to CRMP-2 include lacostamide (Wang et al. 2010) and lantionine ketimine (LK) and its 5-ethyl ester (LKE) (Hensley et al. 2010a, b, 2011). An exciting recent development concerns the use of CRMP-2-derived cell-permeable peptides as potential antinociceptive agents (Brittain et al. 2011; Wilson et al. 2011; Piekarz et al. 2012). All these efforts are complicated by the fact that the detailed biological mechanisms of CRMP-2 function are unknown, and specific ligands binding to it have not been characterized at the structural level.

The crystal structure of CRMP-2 was reported originally by us at ~ 2 Å resolution (Stenmark et al. 2007; Majava et al. 2008). The homotetrameric structure was used to assess the reliability of earlier functional experiments, using e.g. truncated protein constructs in cell culture settings, some of which can have only little real relevance considering the 3D structure of the protein. Also other crystal structures of CRMPs have been refined between 2–3 Å resolution (Deo et al. 2004; Ponnusamy and Lohkamp 2013; Ponnusamy et al. 2014; Liu et al. 2015). While CRMP-2 is an attractive drug target, the previous crystal structures have shown no bound ligand molecules, apart from divalent cations.

Here, we determined the crystal structure of human tetrameric CRMP-2 at the near-atomic 1.25-Å resolution. The data allow to refine the structure at high confidence and, for example, show details for a number of unconventional hydrogen-bonded interactions. Recent functional data are discussed in light of the high-resolution structure. Importantly, the crystal structure reveals possible ligand-binding pockets, one of which changes conformation upon ligand binding. Such data will be useful in further screening

for CRMP-2-affecting small-molecule ligands. All in all, we provide the most accurate structural description of any member of the CRMP family to date.

Methods

Materials

LK/LKE were synthesized as previously described (Hensley et al. 2010b). Human CRMP-2 full-length cDNA was obtained from SGC Stockholm, Sweden.

Protein expression and purification

Recombinant human CRMP-2 (residues 13–490) without the C-terminal tail was expressed and purified essentially as described earlier (Stenmark et al. 2007; Majava et al. 2008). Briefly, His-tagged CRMP-2 was expressed in *E. coli* and purified using Ni affinity and size exclusion chromatography. The protein was concentrated to 13 mg/ml in 20 mM HEPES (pH 7.5), 300 mM NaCl, 10% glycerol (v/v), 1 mM EDTA, 0.5 mM TCEP.

The C-terminal tail of CRMP-2 was also expressed and purified. The expression construct contained an insert coding for residues 491–572, i.e. the last 82 C-terminal residues, of human CRMP-2, obtained by PCR from human CRMP-2 cDNA. The protein was expressed in *E. coli*, being fused to thioredoxin and a His-tag (pDEST-trx vector) (Tsunoda et al. 2005). The protein was expressed with autoinduction (Studier 2005) at +30 °C for 24 h. The over-expressed fusion protein was purified from the cell lysate using Ni affinity. The fusion partner was removed with TEV cleavage and recaptured on the Ni affinity matrix, while the released C-terminal tail of CRMP-2 was further purified with size exclusion chromatography.

Crystallization

For crystallization, CRMP-2 was mixed with 1 mM LKE, and crystals were obtained by vapour diffusion using a well solution consisting of 0.1 M bis-tris (pH 5.5), 22% PEG3350, and 0.2 M ammonium sulphate at +20 °C. For cryoprotection, the crystals were briefly soaked in a buffer containing 1 mM LKE, 0.1 M bis-tris (pH 5.5), 25% PEG3350, 0.2 M ammonium sulphate, and 12% glycerol (v/v). The crystals were cryo-cooled by plunging them into liquid nitrogen.

Structure determination

X-ray diffraction data were collected using synchrotron radiation on the P13 beamline at EMBL/DESY, Hamburg. Data were

processed using XDS (Kabsch 2010). The structure was solved by molecular replacement in Phaser (McCoy et al. 2007), with our earlier structure of human CRMP-2 as template (PDB entry 2GSE (Stenmark et al. 2007)). Refinement was carried out in phenix.refine (Afonine et al. 2012) and model building in Coot (Emsley and Cowtan 2004). Hydrogen atoms were added to the riding positions, and their positions were optimized during refinement. All non-hydrogen atoms were refined anisotropically. The final structure was validated using Molprobit (Davis et al. 2004). Structure analysis was carried out using UCSF Chimera (Pettersen et al. 2004), pdb2pqr (Dolinsky et al. 2004), ccp4 mg (McNicholas et al. 2011), PyMOL, and APBS (Baker et al. 2001). The coordinates and structure factors were deposited at the PDB with the entry code 5LXX.

CD spectroscopy

Folding properties of the isolated C-terminal tail of CRMP-2 were studied by CD spectroscopy. The protein was in a buffer containing 10 mM sodium phosphate at pH 7.5. CD spectra were collected on a Chirascan Plus instrument (Applied Photophysics), and the corresponding buffer baseline was subtracted.

Docking

For docking of small-molecule compounds, the implementation of AutoDock VINA (Trott and Olson 2010) in YASARA (Krieger and Vriend 2014) was the main tool. Docking was carried out for both LK and LKE. Initially, 250 poses were identified in the tetrameric crystal structure for each compound. Thereafter, ten different side chain networks were set up, and 50 poses for each compound were found for each structure. Pockets on CRMP-2 were also identified using MetaPocket (Huang 2009). Furthermore, hot spots for small molecule binding were detected using FTMap (Kozakov et al. 2015).

Sequence analysis

The CRMP-2 C-terminal tail was analysed using various bioinformatics packages, such as PONDR (Xue et al. 2010), ANCHOR (Dosztanyi et al. 2009), IUPred (Dosztanyi et al. 2005), JPred4 (Drozdetskiy et al. 2015), DISOPRED (Ward et al. 2004), PSIPRED (Jones 1999), and DEPP (Iakoucheva et al. 2004). Sequence alignment analysis was done with ESPript (Gouet et al. 1999).

Results and discussion

In this study, we attempted to obtain structural information on complexes between CRMP-2 and the neurological drug

candidates LK/LKE. LK/LKE were, however, not bound to CRMP-2 in the crystal state under the employed crystallization conditions. Among the number of crystals tested, one diffracted to near-atomic resolution, and it was used for high-resolution refinement and will be discussed here. The obtained structure presents accurate details on CRMP-2 and its properties with regard to ligand binding.

Overall characteristics of the CRMP-2 structure

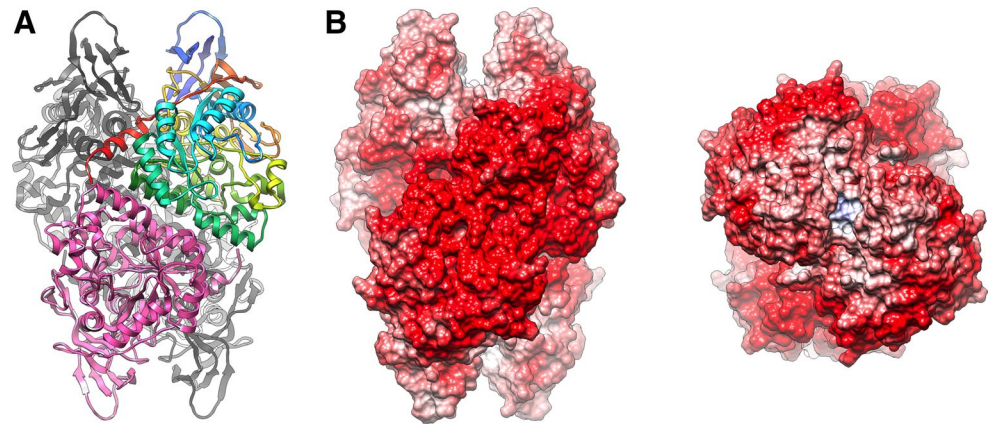
The crystal structure of human CRMP-2 was refined at the near-atomic 1.25-Å resolution (Table 1), from a construct missing the C-terminal tail. While it is likely that the C-terminal tail is disordered, no successful studies thus far have been carried out with full-length CRMP-2 with respect to 3D structure. Interestingly, important functional properties are concentrated within the C-terminal tail, including phosphorylation (Gu et al. 2000) and CaM binding (Zhang et al. 2009); additionally, a peptide from the beginning of the C-terminal tail is being actively studied as having potential nociceptive functions (Quach et al. 2015).

As seen before for CRMP-2, other CRMPs, and DHPases (Abendroth et al. 2002; Deo et al. 2004; Stenmark et al. 2007; Ponnusamy and Lohkamp 2013; Ponnusamy et al. 2014), the structure is a homotetramer with 222 symmetry; each monomer carries a core fold of a TIM barrel (Fig. 1). An additional small domain on top of the barrel could be involved in protein interactions. While the

Table 1 Crystallographic data collection and structure refinement

Data collection	
Beamline	P13/PETRA III
X-ray wavelength (Å)	1.03
Space group	C2
Unit cell dimensions	141.76, 97.04, 92.38, 90, 122.54, 90
Resolution range (Å)	80–1.25 (1.28–1.25)
Completeness (%)	92.7 (57.9)
Redundancy	3.6 (2.3)
R_{sym} (%)	3.9 (77.0)
R_{meas} (%)	4.6 (100.4)
$\langle I/\sigma I \rangle$	15.9 (1.0)
$CC_{1/2}$ (%)	100 (39.9)
Wilson B (Å ²)	19.5
Structure refinement	
$R_{\text{cryst}}/R_{\text{free}}$ (%)	10.4/13.3
rmsd bond lengths (Å)	0.013
rmsd bond angles (°)	1.3
Molprobit score (percentile)	0.92 (99th)
Ramachandran favoured/outliers (%)	97.6/0.0

Fig. 1 The tetrameric structure of CRMP-2. **a** Overall structure. One monomer is coloured with rainbow colours (C terminus, red), one in pink, and two light grey. **b** Left electrostatic surface of the CRMP-2 tetramer. The surface is coloured from red ($-10 K_b T/e_c$) to blue ($+10 K_b T/e_c$). Same view as in **a**. Right electrostatic surface viewed from the top with respect to **a**. The positively charged cavity involves residue Arg400 from two subunits (colour figure online)



DHPase active-site residues are not conserved in CRMPs, a pocket has remained in the structure at the position, where the DHPase active site is. In our earlier structures of CRMP-2, divalent cations were bound to the entrance of this pocket (Stenmark et al. 2007; Majava et al. 2008).

Electrostatic potential calculations of the tetramer reveal large negatively charged patches on the CRMP-2 surface (Fig. 1b). These surfaces could be functional in protein interactions, either with other proteins or with the positively charged C-terminal tails that are missing in the current structure.

Electron density was observed all the way to the last C-terminal residue of the construct, Glu490. Due to the high resolution, a number of small errors, in e.g. side chain rotamers, could be corrected with respect to earlier, lower-resolution structures of CRMP-2, making the current structure the highest-resolution model of any CRMP to date. Several residues were built in alternative conformations, and anisotropic ADP values were refined for all non-hydrogen atoms. A number of aspects of the CRMP-2 structure are discussed further below.

Details for hydrogen atoms

Due to the high resolution and quality of the diffraction data, difference electron density maps show the positions of a large number of hydrogen atoms; allowing to e.g. correctly orient methyl groups of amino acid side chains. Importantly, the position of the hydrogen atom in hydroxyl groups can often be observed. Also unconventional hydrogen bonds, such as C–H...O and C–H... π bonds are frequently visible. Protonation states can also be inferred. Examples of such interesting protein structure details are given in Fig. 2. The fact that hydrogen atoms can be seen in the electron density even at 1.25-Å resolution highlights the excellent quality of the CRMP-2 diffraction data.

Oligomeric packing

The oligomeric interface formed in the current crystal form through crystallographic symmetry was compared to the earlier structures of CRMP-2 (Stenmark et al. 2007; Majava et al. 2008). The interface in the new crystal form is apparently slightly more tightly packed, with a number of new side chain orientations. This tighter packing reveals flexibility at the oligomer interface of CRMPs, and local plasticity could be related to the formation of heterotetramers, which is a documented property within the CRMP family (Wang and Strittmatter 1997; Ponnusamy and Lohkamp 2013).

An unfavourable interaction at the oligomerization interface is presented by a H-bond between the side chains of Glu183 and Glu207; the formation of this contact requires that one of these acidic side chains is protonated. Predictions of pK_a values (Olsson et al. 2011) suggest that Glu207 is protonated in this case. Cys179 lies close to the abovementioned acidic residues, and presents different conformers in the different CRMP-2 structures. These interactions might be important in not making the interface too tight, to allow for heterotetrameric interactions between the CRMP family members.

A salt bridge at the C-terminal end of the construct, and the beginning of the missing C-terminal tail and in the region of the CaM binding segment, is formed to the neighbouring monomer of the tetrameric assembly. Such an interaction is not present in CRMP-1, -4, or -5, which all have hydrophobic residues of the C-terminal tail buried in this pocket (Fig. 3). The C-terminal segment may be involved in regulating tetramerization. Binding of other proteins to these regions, as well as post-translational modifications (PTM), could result in different oligomeric states, as was suggested for CaM (Zhang et al. 2009). It is also possible that binding partners of different CRMPs, as well as PTMs, might regulate the CRMP homo/heterotetramerization balance.

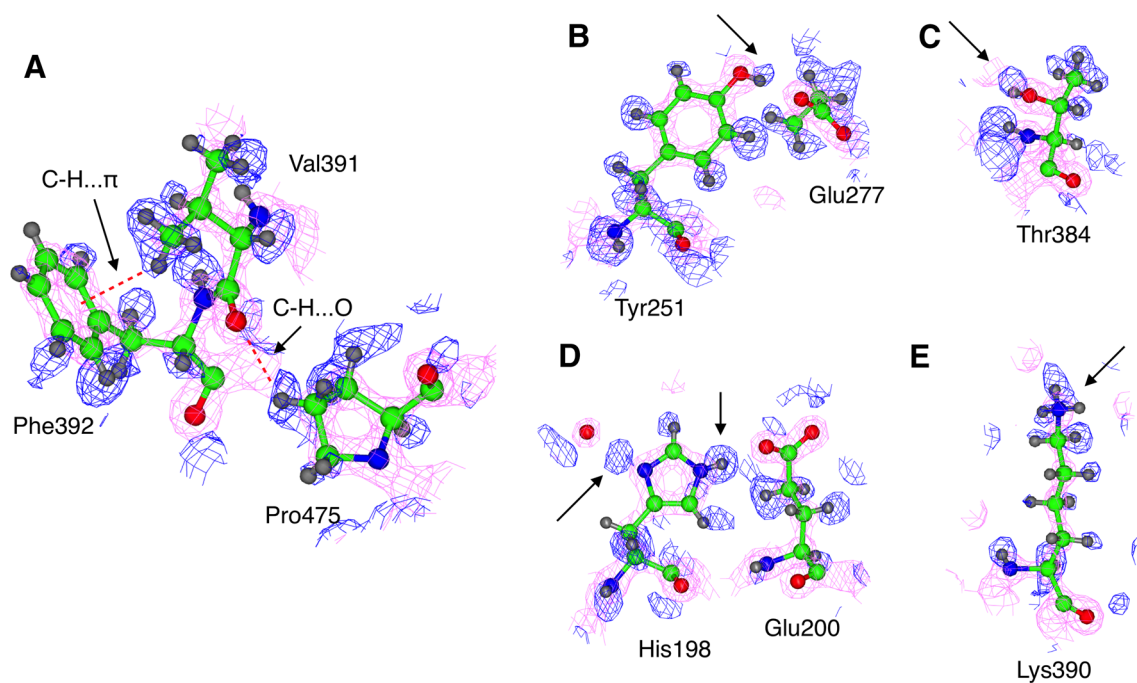


Fig. 2 Selected high-resolution details from the 1.25-Å structure. Electron density maps are shown as follows: $2F_o - F_c$ map at 3.0σ (pink); $F_o - F_c$ at 2.0σ (blue). The maps were calculated after removing hydrogen atoms in the structure. **a** Interactions of Val391 include both a C-H... π bond to the side chain of Phe392 and a C-H...O bond with Pro475 (both shown as red dashed lines). **b** The OH group

(arrow) of Tyr251 is poised to make a hydrogen bond with Glu277. **c** Orientation of the side chain OH group (arrow) can be detected in Thr384. **d** His198 is fully protonated. The exchangeable hydrogens on the side-chain nitrogen atoms are indicated by arrows. **e** The orientation of the terminal NH_3^+ moiety on Lys390 can be determined based on electron density (colour figure online)

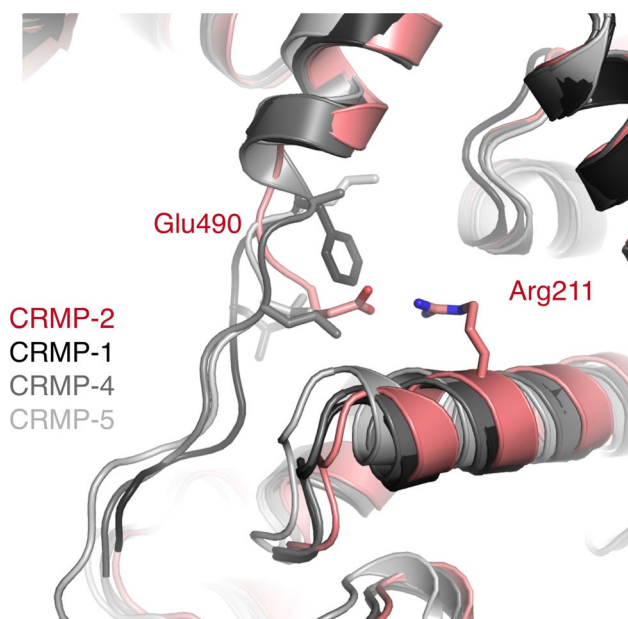


Fig. 3 The oligomer interface in the earlier and current CRMP structures. The salt bridge between Glu490 and Arg211 is a unique feature in CRMP-2. For comparison, the structures of CRMP-1, -4, and -5 are superimposed (grey). Note how each of the latter presents two hydrophobic residues in the same pocket

Surface conservation between human CRMPs

The amino acid conservation between all five human CRMPs was analyzed, in order to highlight possible common functional sites within the family (Fig. 4a). In essence, the areas of the CRMP-2 monomer surface that are fully conserved in all human CRMPs include oligomer interfaces, the outer surface of the small N-terminal domain, and a groove not involved in oligomer interactions in the crystal. For the latter, however, it is clear that this groove might be a binding surface for C-terminal CRMP-2 residues beyond 490 from a neighbouring monomer (Fig. 4b). Also interesting is the conservation of the surface of the small domain, far from oligomer interactions; this may hint at a common functional interaction surface within the CRMPs. Conserved segments are also detected in the C-terminal tail, raising the possibility of common, as of yet unidentified, binding partners for this domain in CRMPs.

Potential binding pockets for small molecules

The main purpose of the current experiments was to obtain a crystal structure of a complex of CRMP-2 and LK/LKE, which were hypothesized to bind directly to CRMP-2

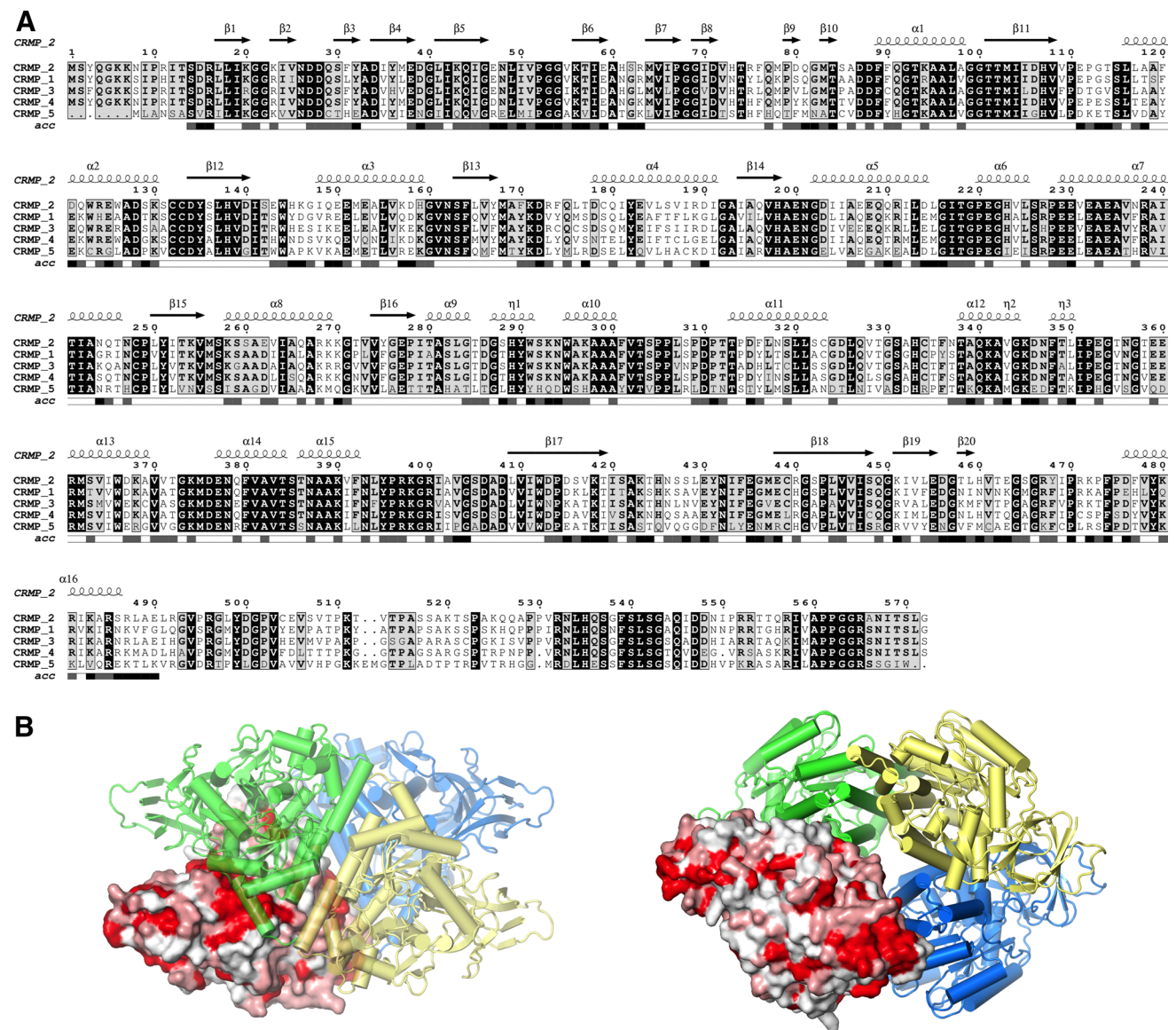


Fig. 4 Conservation of human CRMPs. **a** Sequence alignment of human CRMPs 1–5. The secondary structures inferred from the current crystal structure are shown above the alignment and the accessibility of the residues in CRMP-2 below it. **b** Mapping of the conservation onto the CRMP-2 monomer surface. One monomer of the

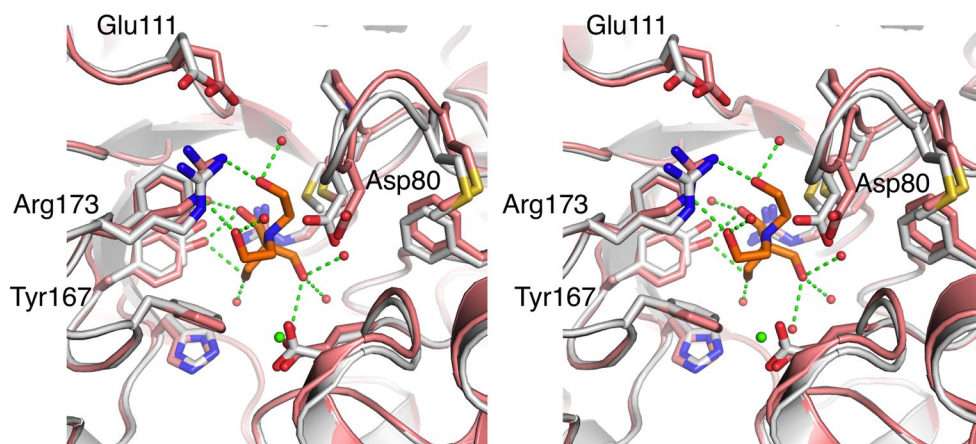
tetramer is shown with a surface, coloured in red for full conservation. Two poses 90° apart are shown. *Left* conservation of the oligomerization interface; *right* conservation of the small domain and a groove possibly binding the C-terminal tail of another subunit (blue) (colour figure online)

(Hensley et al. 2010b). While this did not turn out to be the case in the crystal structure of the truncated variant described here, small molecules from the crystallisation mixture were, indeed, observed to be bound to CRMP-2—at locations, which could be targets for further structure-based drug design experiments. Due to the high resolution of the data from the LKE experiment, these binding modes can be examined in detail.

A number of small conformational changes are observed in the pocket corresponding to the DHPase active site, which in the current structure harbours a bis–tris molecule

(Fig. 5). The two bis–tris binding sites in the asymmetric unit behave slightly differently. In monomer A, the site is clearly only partially occupied, which is linked to alternative conformations of coordinating residues. On the other hand, monomer B is essentially fully occupied, and interacting residues, such as Tyr167, are in one conformation only, which thereby corresponds to the ligand-bound conformation. Furthermore, Tyr167 in our previous unliganded structure is in the unliganded conformation. Water molecules bound to the Tyr167 OH group are also linked to the ligation status of the binding site.

Fig. 5 The ligand-binding pockets in the CRMP-2 crystal structure. Bis-tris binds to the cavity representing the DHPase active site. Conformational changes are observed in the binding cavity, based on liganded (*pink/orange*) and unliganded (*white*) structures. The Ca^{2+} ion in the unliganded structure (2GSE) is shown as a green sphere, and H-bonding interactions of bis-tris as *green dashed lines* (colour figure online)



Differences between unliganded and liganded CRMP-2 are also seen at the edge of the binding pocket. Loops lining the pocket entrance move away in the liganded structure, essentially opening up the cavity for ligand binding (Fig. 5). These loops are at the C-terminal end of the TIM barrel.

The functional relevance of ligand binding to this site is unclear, but our data are the first to show small organic molecule ligand binding to the CRMP pocket corresponding to the DHPase active site. Hence, while enzymatic activity has apparently been lost in CRMP-2, ligand binding activity still exists—and could have a functional role.

At the oligomer interface, Arg400 from two monomers are close to each other, generating strong positive electrostatic potential (Fig. 1b). A ligand is also observed in this pocket, and was modeled as a combination of sulphate and water in alternative conformations. Also several other sulphate ions were detected in electron density on the surface of CRMP-2 (data not shown).

Although LKE is not visible in the crystal, it cannot be ruled out that it would bind to CRMP-2 in solution and/or in vivo. The effects of LKE are generally thought to be mediated through CRMP-2-related pathways (Hensley et al. 2011), and CRMP-2 was identified as a potential binding partner in an affinity-coupled assay (Hensley et al. 2010b). The binding site may e.g. be buried in crystal contacts, or binding may require the C-terminal tail in the context of the full-length protein. It is also possible that a binding site is only revealed in a monomeric or dimeric state. Further studies will definitely be required to answer these questions.

The C-terminal tail

The C-terminal tail of CRMP-2, residues 491–572, was also separately purified. The tail has a pI of 10.9, having a high positive charge, and it is predicted to have a large degree of intrinsic disorder (Fig. 6a, b). Various prediction

algorithms highlighted 3 segments assumed to be possible protein binding sites through disorder–order transitions. Two short β strands are otherwise predicted to be present. Several of the known phosphorylation sites were also predicted based on disorder enhancement methods. The amino acid composition of the CRMP-2 C-terminal tail, on the other hand, lies slightly on the ordered side of the charge/hydrophathy diagram (Fig. 6c), further suggesting possible local folding propensities upon binding to ligands—or to e.g. neighbouring monomers in the tetramer.

The recombinant C-terminal tail alone is disordered, as shown by CD spectroscopy (Fig. 6d). While it is possible that the tail obtains secondary structures in the context of the full-length protein, the result indicates it is not able to independently fold into a globular domain. The results correspond well to protein disorder predictions, and further confirm that the C-terminal tail, which is a significant phosphorylation target, is structurally flexible. All these properties resemble those of the tau protein (Hensley and Kursula 2016).

The contact made to the neighbouring subunit by Glu490, the last residue of the construct in this study, suggests that CRMP-2, like CRMP-1, -4, and -5, can strengthen its tetramerization through the interaction of the C-terminal tail with an apposing monomer (Fig. 3). High-resolution studies of longer constructs of CRMP-2 will be required to confirm this hypothesis in the future. PTMs and interactions in the C-terminal tail could in this way indirectly affect the stability of the entire CRMP-2 homotetramer, or CRMP heterotetramers in general.

Aspects of CRMP-2 post-translational modifications

Phosphorylation is known to be a central phenomenon to regulate CRMP-2 function in the nervous system (Uchida et al. 2009; Varrin-Doyer et al. 2009; Brittain et al. 2012; Wilson et al. 2014; Nagai et al. 2016). Hyperphosphorylation of CRMP-2 has been observed in Alzheimer's disease

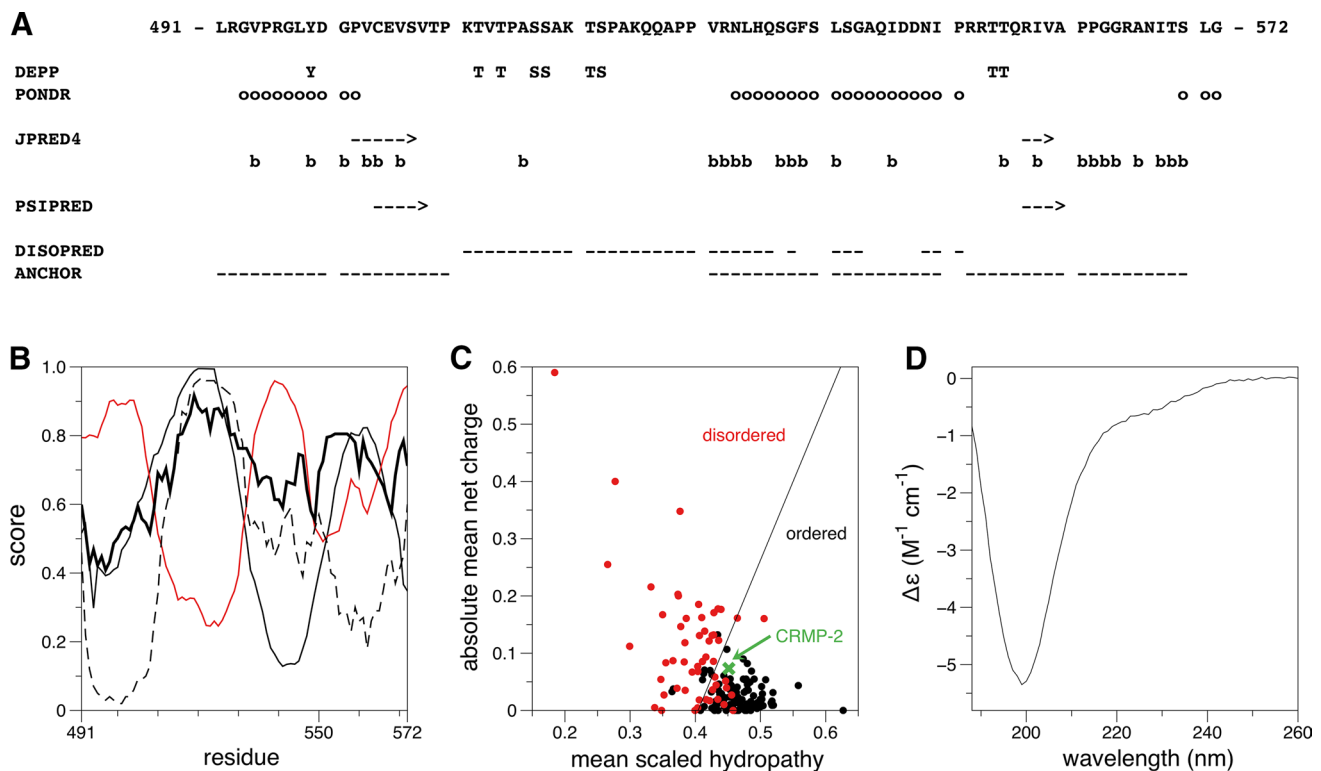


Fig. 6 The C-terminal tail of CRMP-2 is disordered, but with propensity to fold. **a** Bioinformatics predictions on CRMP-2. The following predictions are shown: DEPP, phosphorylation sites based on disorder prediction; PONDR, ordered regions; JPRED4, secondary structure (*top*) and buried regions (*bottom*); PSIPRED, secondary structure; DISOPRED, disordered sites for protein binding; ANCHOR, disordered regions possibly involved in protein interac-

tions. **b** Plots of predictions from ANCHOR (*red*), IUPred (*thick black line*), PONDR (*thin black line*), and DISOPRED (*dashed black line*). ANCHOR predicts protein interaction sites, the other programs protein disorder. **c** Charge/hydropathy analysis places the CRMP-2 C-terminal domain (*green*) at the divider between order and disorder. **d** CD spectrum of the CRMP-2 tail (colour figure online)

(AD) and corresponding mouse models (Gu et al. 2000; Williamson et al. 2011; Khanna et al. 2012; Xing et al. 2016), which together with the homology to tau hints at involvement in AD pathogenesis (Hensley and Kursula 2016).

CRMP-2 has been reported to interact with several proteins, such as neurofibromin (Lin and Hsueh 2008) and tubulin (Fukata et al. 2002). In many of these studies, truncation mutants were used to map binding sites. Based on our earlier CRMP-2 crystal structure determination, we already discussed the reliability of some of these binding sites (Stenmark et al. 2007). Here, we want to further discuss some CRMP-2 PTMs that have been described in the literature or can be found in databases.

While the well-characterized phosphorylation sites of CRMP-2 are located in the C-terminal tail region, a number of additional PTMs have been detected during the recent years in various high-throughput screens. We focused on the PTMs listed and curated on PhosphoSitePlus (Hornbeck et al. 2012), which includes results from both literature and unpublished screens. Figure 7a locates all

the phosphorylation sites of CRMP-2, plus a reported SUMOylation site, on the tetramer structure. It is evident that many of the sites are not surface-exposed (Fig. 7b). Some of them might become accessible upon disruption of the tetramer (Fig. 7c), while others would essentially involve unfolding of CRMP-2. Together with our earlier remarks on carelessly defined binding sites for partner proteins, these observations call for caution when planning experiments based on truncated proteins or PTM results confirmed only by high-throughput screens. Some of the better-characterized PTMs within the crystal structure are discussed below.

Tyr479 is one of the few phosphorylation sites outside the C-terminal tail, which has been characterized. It was suggested that tyrosine kinases might interact with CRMP-2 through a binding site between residues 467–473 through their SH3 domains, as a result of which Tyr479 might become available for phosphorylation (Varrin-Doyer et al. 2009). In the structure, Tyr479 is buried and involved in H-bonds through its hydroxyl group (Fig. 7c, d). Hence, the Y479F mutant used in functional studies (Varrin-Doyer

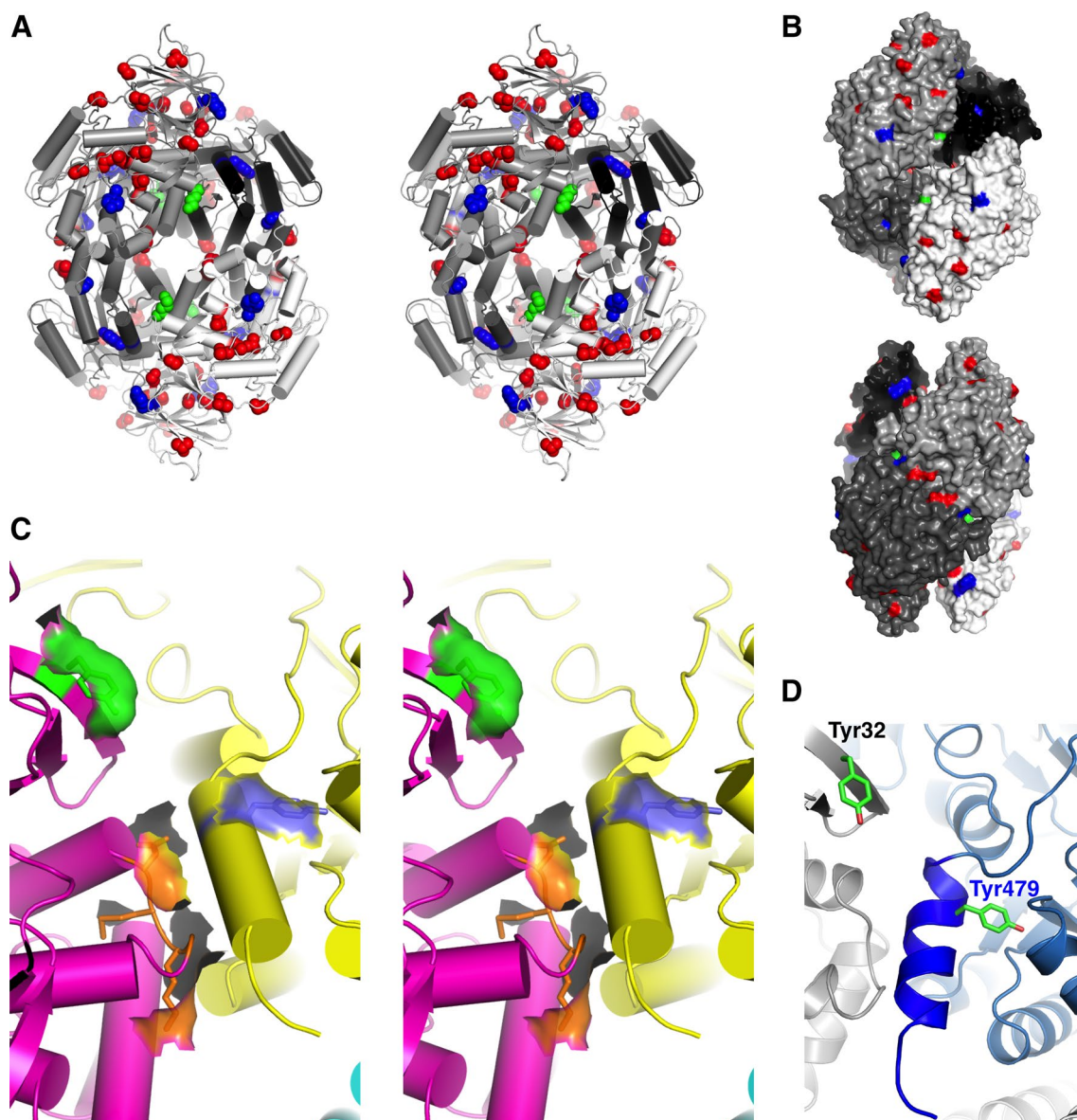


Fig. 7 PTMs from the literature and databases. **a** Location of all CRMP-2 phosphorylation sites in the tetramer, plus the SUMOylation site (stereo view). Ser/Thr phosphorylation, *red*; Tyr phosphorylation, *blue*; SUMOylation, *green*. **b** The same data as surface representation from two orientations 90° apart. Note how only a few sites are on the surface of the tetramer. **c** Zoom-in (stereo view) on the region containing the SUMOylation site (*orange*) from one monomer and

Tyr479 from another (*blue*). Both these sites have very little exposed surface. On the other hand, Tyr32 (*green*) is surface-exposed. The fraction of the surface of the CRMP-2 tetramer corresponding to these residues is shown. **d** A top view of two monomers (*grey* and *blue*) shows how Tyr32 and Tyr479 are close to each other in space in the tetramer (colour figure online)

et al. 2009) would likely be compromised in folding at least locally at this position. It can safely be said that Tyr479 phosphorylation requires major conformational change to occur; such a change could also affect e.g. the oligomeric state of CRMP-2 and the flexibility of the C-terminal region.

Tyr32 phosphorylation by Fyn kinase was suggested to be relevant for Sem3A signaling (Uchida et al. 2009). In the CRMP-2 structure, Tyr32 is solvent-accessible on the surface of the small domain, close to the oligomeric

interface. Interestingly, the last helix of the structure from an apposing monomer lies close by, and this helix would be followed by the C-terminal positively charged tail in the full-length protein. It is possible that phospho-Tyr32 could interact with basic residues in these regions, affecting further protein–protein interactions and CRMP-2 oligomerization. As a matter of fact, Tyr32 and Tyr479 from the apposing subunit lie close in 3D space (Fig. 7c, d), and could be parts of similar regulatory events.

Another reported modification of CRMP-2 is SUMOylation of Lys374 (Dustrude et al. 2013; Ju et al. 2013). Although the original reports stated this site to be surface-exposed, it is in fact buried in the tetrameric assembly (Fig. 7c). Lys374 forms a salt bridge to Asp315 from the same monomer. Thus, very large conformational changes would have to take place for SUMOylation of this site in the CRMP-2 tetramer. On the other hand, dissociation of the tetramer could expose this site. The site is very close to the C-terminal helix of the neighbouring monomer, where Tyr479 also requires conformational change (see above) for its PTM to occur. Furthermore, this helix comprises the possible CaM binding site, and it is possible all these regulatory events are linked.

The antinociceptive peptide being developed based on CRMP-2 (Brittain et al. 2011; Wilson et al. 2011) locates at the end of the folded domain, partially overlapping with the suggested CaM-binding site (Zhang et al. 2009). This segment in CRMP-2 is likely to be important in oligomerization, as can be deduced from crystal structures of other CRMPs (Ponnusamy and Lohkamp 2013; Ponnusamy et al. 2014; Liu et al. 2015), which have been determined for slightly longer constructs (Fig. 3). Taken into account the above-mentioned aspects, the C-terminal helix of the crystal structure, together with the contacts it makes and the C-terminal tail that extends from it, is likely to be a major regulatory site for CRMP-2 oligomerization and function. Pulling away of this helix, for example, could enable new PTMs and disrupt oligomerization. Such a regulatory mechanism has some analogy to the CaM-dependent protein kinases, for example.

Binding of small-molecule compounds to CRMP-2

Surface electrostatics show that the majority of CRMP-2 has a negatively charged surface, with occasional small neutral regions, or even ones with positive charge, such as the sulphate-binding site involving two Arg400 residues from apposing monomers (Fig. 1b). It is possible that these less negatively charged sites provide binding sites for ligands that have negative charge, such as LK/LKE. Lacosamide is another small molecule suggested to act through CRMP-2 directly. It is controversial, whether lacosamide actually binds directly to CRMP-2 or not (Wolff et al. 2012). However, computationally, a binding site was identified (Wang et al. 2010). To obtain information on putative binding sites for LK/LKE on CRMP-2, the full tetramer crystal structure was subjected to docking experiments with both compounds. It is possible that the high concentrations of crystallization reagents, such as sulphate and bis-tris, have prevented LK and LKE binding in the crystal state.

Docking results for LK and LKE were similar, and essentially 3 recurring putative binding site clusters are

highlighted by both compounds in the initial population of 250 binding modes each. These include the above-mentioned possible lacosamide pocket and the bis-tris pocket (the primordial DHPase active site), and a site at the oligomer interface, corresponding to one of the divalent metal binding sites seen before (Majava et al. 2008). Sporadic hits are also found at other oligomerization interfaces, suggesting a possible mode of action related to oligomerization. When using the monomer of CRMP-2 for docking, the two sites detected are the lacosamide and bis-tris pockets (data not shown).

Interestingly, the bis-tris pocket is only found in half of the monomers when docking in the tetramer. The tetramer was built from the crystallographic dimer in the asymmetric unit, and hence, LK/LKE are easily docked into monomer B but not monomer A. Monomer B is the one with full occupancy for bis-tris in the crystal. Indeed, the small

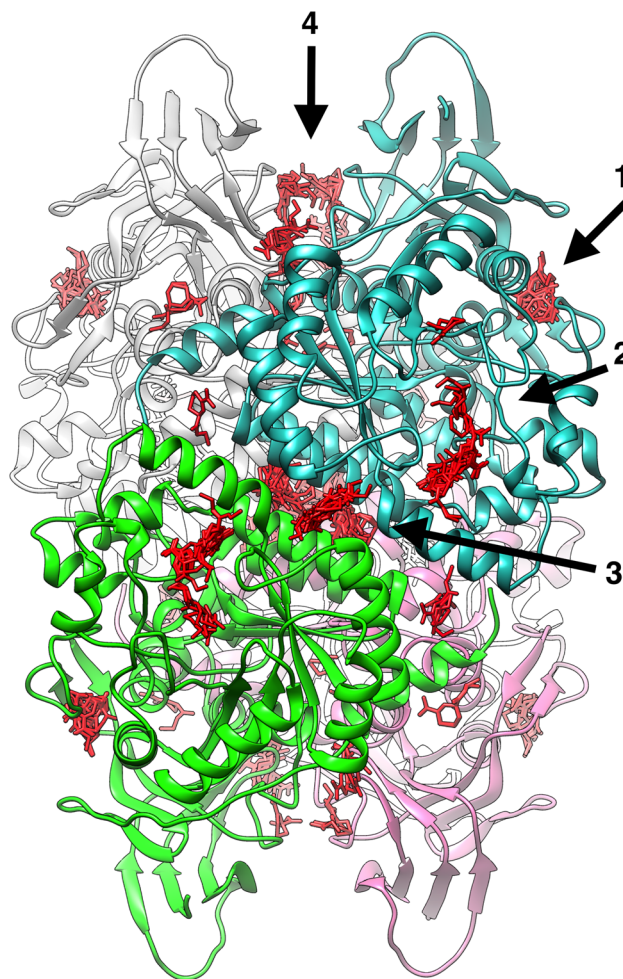


Fig. 8 Docking of LK onto the CRMP-2 tetramer. Different poses of LK are shown in red. Essentially four clusters are identified: 1 the lacosamide pocket, 2 the oligomer interface, 3 the bis-tris pocket, and 4 the groove next to Arg400 from two monomers (colour figure online)

conformational changes related to the occupancy of the bis–tris ligand apparently are large enough to affect docking results. This observation further highlights the usefulness of the current structure, both through its high resolution and through the observed fine conformational changes, for molecular docking approaches.

A more diverse set of potential sites is seen, when side chain networks are altered/optimized on CRMP-2; in addition to the above, oligomer contacts and the C terminus of the structure are detected among the 10 × 50 poses for each compound. The bis–tris pocket is also picked up from all subunits in this case. The groove containing the two Arg400 residues, the area with the highest positive charge on the CRMP-2 surface, is also detected (Fig. 8).

Screening the CRMP-2 structure with the program Metapocket identified both the bis–tris binding site as well as the predicted lacosamide binding site. On the other hand, FTMap identified the bis–tris pocket in all four subunits as a potential hot spot for several small-molecule compounds, and clusters of binding sites were also detected at oligomer interfaces.

All the current data point towards a property of CRMP-2 to be able to bind small molecules at different sites. The physiologically/pharmacologically relevant binding sites, the identity of the putative ligands, and their respective effects on CRMP-2 structure and function, still remain to be determined. The conformational flexibility related to bis–tris binding is an example of a process that is difficult to predict.

Conclusions

The CRMPs are an intriguing group of proteins with homology to the DHPases, but with no well-defined physiological function at the molecular level. CRMP-2 is known to be important for axonal pathfinding, and it is heavily being studied as a drug target, but all structure–function data to date are rather inconclusive. Its possible biomedical roles, including those related to nociception, further raise interest in CRMP-2 and the entire CRMP family. Our high-resolution crystallographic data should provide very useful in structure-guided drug design efforts in the future, both for CRMP-2 and for all the other CRMPs. Furthermore, high-resolution structural data on CRMP–ligand protein complexes, as well as on full-length CRMPs, are eagerly anticipated.

Acknowledgements We wish to thank SGC Stockholm for providing the CRMP-2 cDNA, the Biocenter Oulu crystallization facility for excellent infrastructure, and EMBL-Hamburg/DESY for beamtime and outstanding beamline support. This research was funded by the Academy of Finland (PK), the Sigrid Jusélius Foundation (Finland) (PK), the Emil Aaltonen Foundation (Finland) (PK), Helse Vest

(Bergen, Norway) (AB), and the Research and Science Foundation of the City of Hamburg (Germany) (PK). KH is funded for CRMP-2 research through the National Institutes of Health (NS082283 and NS093594).

Compliance with ethical standards

Conflict of interest KH is the inventor on US patent 7,683,055 (other patents pending) covering composition and use of LK derivatives including LKE and holds equity in a company engaged in commercial development of the technology.

Research involving human participants and/or animals This article does not contain any studies with human participants or animals performed by any of the authors.

References

- Abendroth J, Niefind K, Schomburg D (2002) X-ray structure of a dihydropyrimidinase from *Thermus* sp. at 1.3 Å resolution. *J Mol Biol* 320:143–156
- Afonine PV, Grosse-Kunstleve RW, Echols N, Headd JJ, Moriarty NW, Mustyakimov M, Terwilliger TC, Urzhumtsev A, Zwart PH, Adams PD (2012) Towards automated crystallographic structure refinement with phenix.refine. *Acta Crystallogr D Biol Crystallogr* 68:352–367
- Astle MV, Ooms LM, Cole AR, Binge LC, Dyson JM, Layton MJ, Petratos S, Sutherland C, Mitchell CA (2011) Identification of a proline-rich inositol polyphosphate 5-phosphatase (PIPP)*collapsin response mediator protein 2 (CRMP2) complex that regulates neurite elongation. *J Biol Chem* 286:23407–23418
- Baker NA, Sept D, Joseph S, Holst MJ, McCammon JA (2001) Electrostatics of nanosystems: application to microtubules and the ribosome. *Proc Natl Acad Sci USA* 98:10037–10041
- Benedict JW, Getty AL, Wishart TM, Gillingwater TH, Pearce DA (2009) Protein product of CLN6 gene responsible for variant late-onset infantile neuronal ceroid lipofuscinosis interacts with CRMP-2. *J Neurosci Res* 87:2157–2166
- Brittain JM, Duarte DB, Wilson SM, Zhu W, Ballard C, Johnson PL, Liu N, Xiong W, Ripsch MS, Wang Y, Fehrenbacher JC, Fitz SD, Khanna M, Park CK, Schmutzler BS, Cheon BM, Due MR, Brustovetsky T, Ashpole NM, Hudmon A, Meroueh SO, Hingtgen CM, Brustovetsky N, Ji RR, Hurley JH, Jin X, Shekhar A, Xu XM, Oxford GS, Vasko MR, White FA, Khanna R (2011) Suppression of inflammatory and neuropathic pain by uncoupling CRMP-2 from the presynaptic Ca(2+)(+) channel complex. *Nat Med* 17:822–829
- Brittain JM, Wang Y, Eruvvetere O, Khanna R (2012) Cdk5-mediated phosphorylation of CRMP-2 enhances its interaction with Cav2.2. *FEBS Lett* 586:3813–3818
- Chi XX, Schmutzler BS, Brittain JM, Wang Y, Hingtgen CM, Nicol GD, Khanna R (2009) Regulation of N-type voltage-gated calcium channels (Cav2.2) and transmitter release by collapsin response mediator protein-2 (CRMP-2) in sensory neurons. *J Cell Sci* 122:4351–4362
- Davis IW, Murray LW, Richardson JS, Richardson DC (2004) MOLPROBITY: structure validation and all-atom contact analysis for nucleic acids and their complexes. *Nucleic Acids Res* 32:W615–W619
- Deo RC, Schmidt EF, Elhabazi A, Togashi H, Burley SK, Strittmatter SM (2004) Structural bases for CRMP function in plexin-dependent semaphorin3A signaling. *EMBO J* 23:9–22

- Dolinsky TJ, Nielsen JE, McCammon JA, Baker NA (2004) PDB2PQR: an automated pipeline for the setup of Poisson–Boltzmann electrostatics calculations. *Nucleic Acids Res* 32:W665–W667
- Dosztanyi Z, Csizmok V, Tompa P, Simon I (2005) IUPred: web server for the prediction of intrinsically unstructured regions of proteins based on estimated energy content. *Bioinformatics* 21:3433–3434
- Dosztanyi Z, Meszaros B, Simon I (2009) ANCHOR: web server for predicting protein binding regions in disordered proteins. *Bioinformatics* 25:2745–2746
- Drozdetskiy A, Cole C, Procter J, Barton GJ (2015) JPred4: a protein secondary structure prediction server. *Nucleic Acids Res* 43:W389–W394
- Dustrude ET, Wilson SM, Ju W, Xiao Y, Khanna R (2013) CRMP2 protein SUMOylation modulates Nav1.7 channel trafficking. *J Biol Chem* 288:24316–24331
- Emsley P, Cowtan K (2004) Coot: model-building tools for molecular graphics. *Acta Crystallogr D Biol Crystallogr* 60:2126–2132
- Fukata Y, Itoh TJ, Kimura T, Menager C, Nishimura T, Shiromizu T, Watanabe H, Inagaki N, Iwamatsu A, Hotani H, Kaibuchi K (2002) CRMP-2 binds to tubulin heterodimers to promote microtubule assembly. *Nat Cell Biol* 4:583–591
- Gouet P, Courcelle E, Stuart DI, Metz F (1999) ESPript: analysis of multiple sequence alignments in PostScript. *Bioinformatics* 15:305–308
- Gu Y, Hamajima N, Ihara Y (2000) Neurofibrillary tangle-associated collapsin response mediator protein-2 (CRMP-2) is highly phosphorylated on Thr-509, Ser-518, and Ser-522. *Biochemistry* 39:4267–4275
- Hensley K, Kursula P (2016) Collapsin response mediator protein-2 (CRMP2) is a plausible etiological factor and potential therapeutic target in Alzheimer's disease: comparison and contrast with microtubule-associated protein tau. *J Alzheimers Dis* 53:1–14
- Hensley K, Venkova K, Christov A (2010a) Emerging biological importance of central nervous system lanthionines. *Molecules* 15:5581–5594
- Hensley K, Christov A, Kamat S, Zhang XC, Jackson KW, Snow S, Post J (2010b) Proteomic identification of binding partners for the brain metabolite lanthionine ketimine (LK) and documentation of LK effects on microglia and motoneuron cell cultures. *J Neurosci* 30:2979–2988
- Hensley K, Venkova K, Christov A, Gunning W, Park J (2011) Collapsin response mediator protein-2: an emerging pathologic feature and therapeutic target for neurodegeneration. *Mol Neurobiol* 43:180–191
- Hornbeck PV, Kornhauser JM, Tkachev S, Zhang B, Skrzypek E, Murray B, Latham V, Sullivan M (2012) PhosphoSitePlus: a comprehensive resource for investigating the structure and function of experimentally determined post-translational modifications in man and mouse. *Nucleic Acids Res* 40:D261–D270
- Hou ST, Jiang SX, Aylsworth A, Cooke M, Zhou L (2013) Collapsin response mediator protein 3 deacetylates histone H4 to mediate nuclear condensation and neuronal death. *Sci Rep* 3:1350
- Huang B (2009) MetaPocket: a meta approach to improve protein ligand binding site prediction. *OMICS* 13:325–330
- Iakoucheva LM, Radivojac P, Brown CJ, O'Connor TR, Sikes JG, Obradovic Z, Dunker AK (2004) The importance of intrinsic disorder for protein phosphorylation. *Nucleic Acids Res* 32:1037–1049
- Jones DT (1999) Protein secondary structure prediction based on position-specific scoring matrices. *J Mol Biol* 292:195–202
- Ju W, Li Q, Wilson SM, Brittain JM, Meroueh L, Khanna R (2013) SUMOylation alters CRMP2 regulation of calcium influx in sensory neurons. *Channels (Austin)* 7:153–159
- Kabsch W (2010) XDS. *Acta Crystallogr D Biol Crystallogr* 66:125–132
- Khanna R, Wilson SM, Brittain JM, Weimer J, Sultana R, Butterfield A, Hensley K (2012) Opening Pandora's jar: a primer on the putative roles of CRMP2 in a panoply of neurodegenerative, sensory and motor neuron, and central disorders. *Future Neurol* 7:749–771
- Kimura T, Watanabe H, Iwamatsu A, Kaibuchi K (2005) Tubulin and CRMP-2 complex is transported via Kinesin-1. *J Neurochem* 93:1371–1382
- Kozakov D, Grove LE, Hall DR, Bohnuud T, Mottarella SE, Luo L, Xia B, Beglov D, Vajda S (2015) The FTMap family of web servers for determining and characterizing ligand-binding hot spots of proteins. *Nat Protoc* 10:733–755
- Krieger E, Vriend G (2014) YASARA View—molecular graphics for all devices—from smartphones to workstations. *Bioinformatics* 30:2981–2982
- Lee S, Kim JH, Lee CS, Kim JH, Kim Y, Heo K, Ihara Y, Goshima Y, Suh PG, Ryu SH (2002) Collapsin response mediator protein-2 inhibits neuronal phospholipase D(2) activity by direct interaction. *J Biol Chem* 277:6542–6549
- Lin YL, Hsueh YP (2008) Neurofibromin interacts with CRMP-2 and CRMP-4 in rat brain. *Biochem Biophys Res Commun* 369:747–752
- Liu SH, Huang SF, Hsu YL, Pan SH, Chen YJ, Lin YH (2015) Structure of human collapsin response mediator protein 1: a possible role of its C-terminal tail. *Acta Crystallogr F Struct Biol Commun* 71:938–945
- Majava V, Loytynoja N, Chen WQ, Lubec G, Kursula P (2008) Crystal and solution structure, stability and post-translational modifications of collapsin response mediator protein 2. *FEBS J* 275:4583–4596
- Makihara H, Nakai S, Ohkubo W, Yamashita N, Nakamura F, Kiyonari H, Shioi G, Jitsuki-Takahashi A, Nakamura H, Tanaka F, Akase T, Kolattukudy P, Goshima Y (2016) CRMP1 and CRMP2 have synergistic but distinct roles in dendritic development. *Genes Cells* 21:994–1005
- McCoy AJ, Grosse-Kunstleve RW, Adams PD, Winn MD, Storoni LC, Read RJ (2007) Phaser crystallographic software. *J Appl Crystallogr* 40:658–674
- McNicholas S, Potterton E, Wilson KS, Noble ME (2011) Presenting your structures: the CCP4 mg molecular-graphics software. *Acta Crystallogr D Biol Crystallogr* 67:386–394
- Nagai J, Owada K, Kitamura Y, Goshima Y, Ohshima T (2016) Inhibition of CRMP2 phosphorylation repairs CNS by regulating neurotrophic and inhibitory responses. *Exp Neurol* 277:283–295
- Nakamura H, Yamashita N, Kimura A, Kimura Y, Hirano H, Makihara H, Kawamoto Y, Jitsuki-Takahashi A, Yonezaki K, Takase K, Miyazaki T, Nakamura F, Tanaka F, Goshima Y (2016) Comprehensive behavioral study and proteomic analyses of CRMP2-deficient mice. *Genes Cells* 21:1059–1079
- Olsson MH, Sondergaard CR, Rostkowski M, Jensen JH (2011) PROPKA3: consistent treatment of internal and surface residues in empirical pKa predictions. *J Chem Theory Comput* 7:525–537
- Pettersen EF, Goddard TD, Huang CC, Couch GS, Greenblatt DM, Meng EC, Ferrin TE (2004) UCSF Chimera—a visualization system for exploratory research and analysis. *J Comput Chem* 25:1605–1612
- Piekarz AD, Due MR, Khanna M, Wang B, Ripsch MS, Wang R, Meroueh SO, Vasko MR, White FA, Khanna R (2012) CRMP-2 peptide mediated decrease of high and low voltage-activated calcium channels, attenuation of nociceptor excitability, and antinociception in a model of AIDS therapy-induced painful peripheral neuropathy. *Mol Pain* 8:54
- Ponnusamy R, Lohkamp B (2013) Insights into the oligomerization of CRMPs: crystal structure of human collapsin response mediator protein 5. *J Neurochem* 125:855–868

- Ponnusamy R, Lebedev AA, Pahlow S, Lohkamp B (2014) Crystal structure of human CRMP-4: correction of intensities for lattice-translocation disorder. *Acta Crystallogr D Biol Crystallogr* 70:1680–1694
- Quach TT, Honnorat J, Kolattukudy PE, Khanna R, Duchemin AM (2015) CRMPs: critical molecules for neurite morphogenesis and neuropsychiatric diseases. *Mol Psychiatry* 20:1037–1045
- Stenmark P, Ogg D, Flodin S, Flores A, Kotenyova T, Nyman T, Nordlund P, Kursula P (2007) The structure of human collapsin response mediator protein 2, a regulator of axonal growth. *J Neurochem* 101:906–917
- Studier FW (2005) Protein production by auto-induction in high density shaking cultures. *Protein Expr Purif* 41:207–234
- Trott O, Olson AJ (2010) AutoDock Vina: improving the speed and accuracy of docking with a new scoring function, efficient optimization, and multithreading. *J Comput Chem* 31:455–461
- Tsunoda Y, Sakai N, Kikuchi K, Katoh S, Akagi K, Miura-Ohnuma J, Tashiro Y, Murata K, Shibuya N, Katoh E (2005) Improving expression and solubility of rice proteins produced as fusion proteins in *Escherichia coli*. *Protein Expr Purif* 42:268–277
- Uchida Y, Ohshima T, Yamashita N, Ogawara M, Sasaki Y, Nakamura F, Goshima Y (2009) Semaphorin3A signaling mediated by Fyn-dependent tyrosine phosphorylation of collapsin response mediator protein 2 at tyrosine 32. *J Biol Chem* 284:27393–27401
- Varrin-Doyer M, Vincent P, Cavagna S, Auvergnon N, Noraz N, Rogemond V, Honnorat J, Moradi-Ameli M, Giraudon P (2009) Phosphorylation of collapsin response mediator protein 2 on Tyr-479 regulates CXCL12-induced T lymphocyte migration. *J Biol Chem* 284:13265–13276
- Wang LH, Strittmatter SM (1997) Brain CRMP forms heterotetramers similar to liver dihydropyrimidinase. *J Neurochem* 69:2261–2269
- Wang Y, Brittain JM, Jarecki BW, Park KD, Wilson SM, Wang B, Hale R, Meroueh SO, Cummins TR, Khanna R (2010) In silico docking and electrophysiological characterization of iacosamide binding sites on collapsin response mediator protein-2 identifies a pocket important in modulating sodium channel slow inactivation. *J Biol Chem* 285:25296–25307
- Ward JJ, McGuffin LJ, Bryson K, Buxton BF, Jones DT (2004) The DISOPRED server for the prediction of protein disorder. *Bioinformatics* 20:2138–2139
- Williamson R, van Aalten L, Mann DM, Platt B, Plattner F, Bedford L, Mayer J, Howlett D, Usardi A, Sutherland C, Cole AR (2011) CRMP2 hyperphosphorylation is characteristic of Alzheimer's disease and not a feature common to other neurodegenerative diseases. *J Alzheimers Dis* 27:615–625
- Wilson SM, Brittain JM, Piekarz AD, Ballard CJ, Ripsch MS, Cummins TR, Hurley JH, Khanna M, Hammes NM, Samuels BC, White FA, Khanna R (2011) Further insights into the antinociceptive potential of a peptide disrupting the N-type calcium channel-CRMP-2 signaling complex. *Channels (Austin)* 5:449–456
- Wilson SM, Ki Yeon S, Yang XF, Park KD, Khanna R (2014) Differential regulation of collapsin response mediator protein 2 (CRMP2) phosphorylation by GSK3 α and CDK5 following traumatic brain injury. *Front Cell Neurosci* 8:135
- Wolff C, Carrington B, Varrin-Doyer M, Vandendriessche A, Van der Perren C, Famelart M, Gillard M, Foerch P, Rogemond V, Honnorat J, Lawson A, Miller K (2012) Drug binding assays do not reveal specific binding of iacosamide to collapsin response mediator protein 2 (CRMP-2). *CNS Neurosci Ther* 18:493–500
- Xing H, Lim YA, Chong JR, Lee JH, Aarsland D, Ballard CG, Francis PT, Chen CP, Lai MK (2016) Increased phosphorylation of collapsin response mediator protein-2 at Thr514 correlates with beta-amyloid burden and synaptic deficits in Lewy body dementias. *Mol Brain* 9:84
- Xue B, Dunbrack RL, Williams RW, Dunker AK, Uversky VN (2010) PONDR-FIT: a meta-predictor of intrinsically disordered amino acids. *Biochim Biophys Acta* 1804:996–1010
- Zhang Z, Majava V, Greffier A, Hayes RL, Kursula P, Wang KK (2009) Collapsin response mediator protein-2 is a calmodulin-binding protein. *Cell Mol Life Sci* 66:526–536
- Zhang H, Kang E, Wang Y, Yang C, Yu H, Wang Q, Chen Z, Zhang C, Christian KM, Song H, Ming GL, Xu Z (2016) Brain-specific Crmp2 deletion leads to neuronal development deficits and behavioural impairments in mice. *Nat Commun* 7:11773